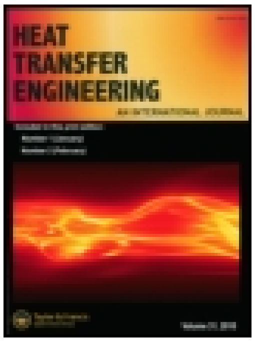


Heat Transfer Engineering

ISSN: (Print) (Online) Journal homepage: https://www.tandfonline.com/loi/uhte20

# Experimental Investigation of the Isothermal Pressure Drops in Mini-Elbows

Hou Kuan Tam, Jia Qi Ji, Lap Mou Tam & Afshin J. Ghajar

**To cite this article:** Hou Kuan Tam, Jia Qi Ji, Lap Mou Tam & Afshin J. Ghajar (2022): Experimental Investigation of the Isothermal Pressure Drops in Mini-Elbows, Heat Transfer Engineering, DOI: 10.1080/01457632.2022.2140634

**To link to this article:** https://doi.org/10.1080/01457632.2022.2140634

Published online: 07 Nov 2022.

HEAT TRANSFER ENGINEERING
https://doi.org/10.1080/01457632.2022.2140634

Taylor & Francis
Taylor & Francis Group

Check for updates

# Experimental Investigation of the Isothermal Pressure Drops in Mini-Elbows

Hou Kuan Tam[a], Jia Qi Ji[a], Lap Mou Tam[a,b], and Afshin J. Ghajar[c]

[a]Department of Electromechanical Engineering, Faculty of Science and Technology, University of Macau, Macau, China; [b]Institute for the Development and Quality, Macau, China; [c]School of Mechanical and Aerospace Engineering, Oklahoma State University, Stillwater, Oklahoma, USA

**ABSTRACT**
An experimental setup was built in this study to measure the pressure drop for the horizontal mini-scale elbows under the isothermal boundary condition. Six stainless steel mini-elbows with various bending angles (45° and 90°) and inner diameters (0.6 mm to 4.5 mm) were used as the test section. The experimental setup was verified by comparing the current horizontal straight tube data with the well-known correlations. The Reynolds number range for this study was around 800 to 10,000. The experimental results clearly showed the effect of diameter and angle on the loss coefficient for the 45° and 90° elbows in the entire Reynolds number range. A critical region was shown to be obvious in the 45° elbows than that in the 90° elbows. Basically, the traditional fixed loss coefficient and the 2-K and 3-K methods did not predict the loss coefficients of the 45° and 90° mini-elbows with good accuracy. Therefore, an accurate correlation was developed for different diameters and angles of mini-elbows and the majority of loss coefficients data was predicted within an accuracy of ±20%.

**ARTICLE HISTORY**

## Introduction

For a pipe system, the friction loss can be classified as major loss and minor loss. The major loss is the friction loss due to the length of pipe and the minor loss is the friction loss due to the fittings such as pipe entrance or exit, bends, elbows, and valves. Minor losses are generally measured experimentally and usually expressed in terms of the loss coefficient, $K_L$ (also called the resistance coefficient). In general, the loss coefficient depends on the geometry of the fitting and the Reynolds number. However, for the traditional macro-scale fittings, the loss coefficient tends to be independent of the Reynolds number because the flow in those fittings is practically in the turbulent region. Loss coefficients of various pipe fittings for turbulent flow can be found in the textbooks of White [1] and Cengel and Cimbala [2].

One of the fittings in a pipe system for the change in flow direction without a change in diameter is called a bend or an elbow. The minor loss in an elbow is due to flow separation from the inner wall and the resulting swirling secondary flows. Spedding et al. [3] stated that the fluid dynamics in elbow bends proved to be complex, with separation and boundary layer effects causing downstream flow to exhibit cyclic characteristics that had not been amenable to theoretical treatment. For this reason, the experimental analysis for the fluid flow inside the elbows is required. White [1] tabulates the loss coefficients for the 45° and 90° screwed elbows (0.5 to 4 inches in diameter) and flanged elbows (1 to 20 inches in diameter). For example, the loss coefficients for the one-inch 45° and 90° long-radius flanged elbows are given as 0.21 and 0.4, respectively. From Cengel and Cimbala [2], the loss coefficient for the 90° smooth flanged elbow is 0.3. Besides these fixed loss coefficient values which are independent of the Reynolds number, Darby and Chbabra [4] stated that loss coefficient for different fittings could also be correlated in terms of Reynolds number by 2-K and 3-K methods. The 2-K method by Hooper [5, 6] is based on experimental data from a variety of valves and fittings over a wide range of Reynolds numbers. The two K constants, $K_1$ and $K_\infty$, are used in the 2-K correlation. The effect of both the Reynolds number and scale (fitting size) is reflected in the expression for the loss coefficient. However, Darby and Chbabra [4] stated that the scaling of pipe size is not accurately reflected by the 2-K method.

CONTACT Dr. Hou Kuan Tam hktam@um.edu.mo Department of Electromechanical Engineering, Faculty of Science and Technology, University of Macau, Avenida da Universidade, Taipa, Macau, China

## Nomenclature

| | |
|---|---|
| $D_i$ | inside diameter of the test section (tube), m |
| $D_o$ | outside diameter of the test section (tube), m |
| $D_{i,in}$ | internal diameter used in Eq. (1), in |
| $D_{n,in}$ | nominal diameter used in Eq. (2), in |
| $D_{i,mm}$ | internal diameter used in Eq. (3), mm |
| f | fully developed friction factor coefficient (Darcy friction factor), $(= 2\cdot D_i \cdot \Delta P/\rho \cdot L \cdot V^2)$, dimensionless |
| $K_1$ | parameter of Eq. (1) and Eq. (2), dimensionless |
| $K_\infty$ | parameter of Eq. (1), dimensionless |
| $K_i$ | parameter of Eq. (2), dimensionless |
| $K_d$ | parameter of Eq. (2), dimensionless |
| $K_L$ | loss coefficient, $(= \Delta p/\frac{1}{2}\cdot \rho \cdot V^2)$, dimensionless |
| L | length of the straight tube, m |
| Q | Flow rate, $m^3/s$ |
| R | curvature radius for the elbow, mm |
| Re | local bulk Reynolds number $(= \rho \cdot V \cdot D_{i}/\mu_b)$, dimensionless |
| $T_b$ | local bulk temperature of the test fluid, °C |
| V | average velocity in the test section, m/s |
| x | local axial distance along the test section from the inlet, m |

***Greek symbols***

| | |
|---|---|
| $\Delta P$ | pressure drop, Pa |
| $\alpha$ | angle of elbow, ° |
| $\varepsilon_{avg}$ | average roughness height, $\mu m$ |
| $\mu_b$ | absolute viscosity of the test fluid evaluated at $T_b$, Pa·s |
| $\rho$ | density of the test fluid evaluated at $T_b$, $kg/m^3$ |

Due to the 2-K's drawback, Darby [7] developed a more accurate "3-K" correlation for the calculation of loss coefficient. In that correlation, the values of the three K constants, $K_1$, $K_i$, and $K_d$ used for various valves and fittings are listed in Darby [7] and Darby and Chbabra [4]. For the classical size elbows, some recent experiments were also conducted to study the single-phase flow or multiphase flow pressure drop across the elbows. Al-Tameemi and Ricco [8] investigated the pressure loss coefficient of 90° sharp-angled miter elbows by using the fluid of water and air in the range of Reynolds number between 500 and 60,000. The 90° elbows with three diameters of 11 mm, 16 mm, and 21 mm were constructed by cutting and gluing two acrylic pieces at 45°. The results showed that the coefficient decreased sharply with the Reynolds number up to about Re of 20,000 and, at higher Reynolds numbers, to approach a constant of 0.9. Based on the elbow data, the empirical loss coefficient correlation was developed in terms of straight-pipe friction factor at the same Reynolds number. Gasljevic and Matthys [9] conducted experiments for studying the drag-reducing flow in curved pipes and 90° elbows. Two elbows of different sizes and types (a 12.7 mm threaded elbow and a 152.4 mm welded elbow) were tested in turbulent flow of both water and drag-reducing surfactant solution. As a result, the pressure drop coefficient of the 12.7 mm elbow for the surfactant solution was practically the same as for water, i.e., about 0.8. For the 152.4 mm elbow, about 40% drag reduction was measured. Spedding et al. [10] experimentally studied a three-phase fluid flow through a vertical upward to horizontal 90° elbow bend with an internal diameter of 26 mm and the curvature ratio of $R/D_i = 0.654$. The results were more complex than corresponding single- and two-phase data. The elbow bend pressure drop was best presented as the equivalent length to diameter ratio using the actual total pressure drop in the vertical inlet tangent leg. In that study, it was stated that the single-phase effect of the bend pressure drop was needed to quantify before proceeding to any multi-phase study.

Due to the rapid development of technology, the miniaturization of devices and components is increasing in many applications. Whether it is in the application of miniature heat exchangers, fuel cells, pumps, compressors, turbines, sensors, or artificial blood vessels, a sound understanding of fluid flow in mini-scale fittings such as mini-elbow is required in different flow regimes. However, seldom experimental studies investigated the single-phase friction factor characteristics in the mini- or micro-scale elbows, especially, the 45° mini-elbow. Hsu et al. [11] conducted experimental studies for the single-phase frictional characteristics and flow patterns of 90° bends. The two-glass bends had inner diameter ($D_i$) of 5.5 and 9.5 mm with tube curvature ratios ($R/D_i$) of 2.7 and 2.1, respectively. The bends were installed in either an upward, horizontal, or downward arrangement. For the single-phase flow, the bend friction factor was always greater than that of the straight tubes at the same liquid Reynolds number. On the other hand, the friction factor values for the 9.5 mm bend with a smaller curvature ratio were greater than those of the 5.5 mm bend. However, the loss coefficient was neglected in that study.

Autee and Giri [12] studied the two-phase flow pressure drop in the mini-bends with the diameters of 6.4 mm and 8.4 mm and different bending angles of the range 90° to 180°. The curvature ratio ($R/D_i$) corresponding to the two diameters was 5.48 and 7.11,

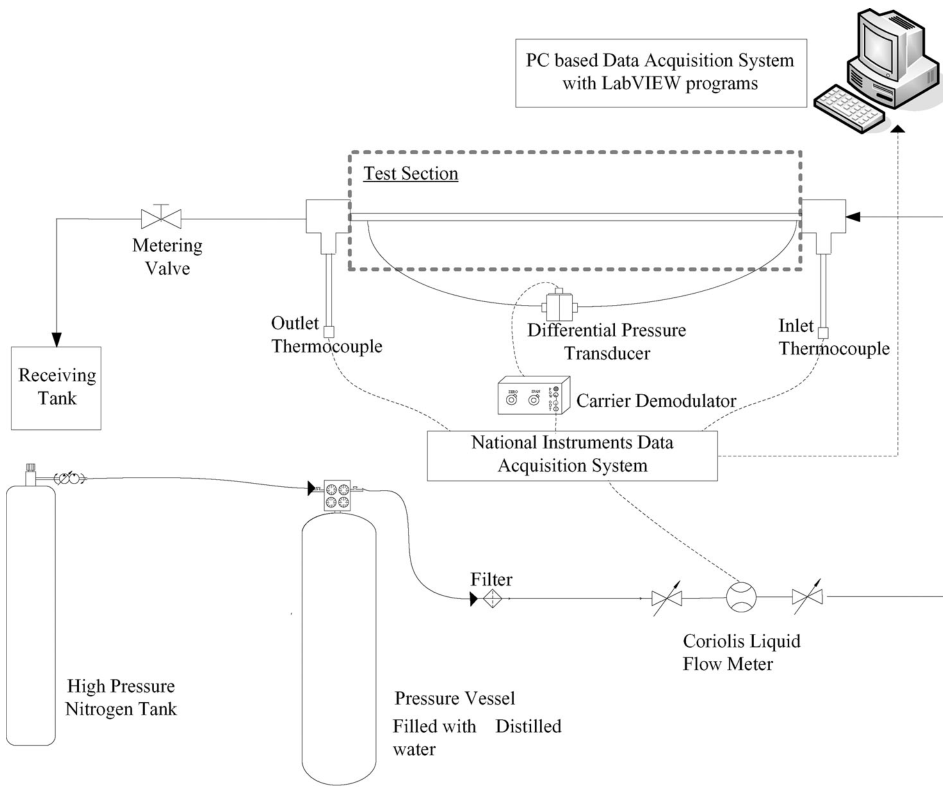


(a)

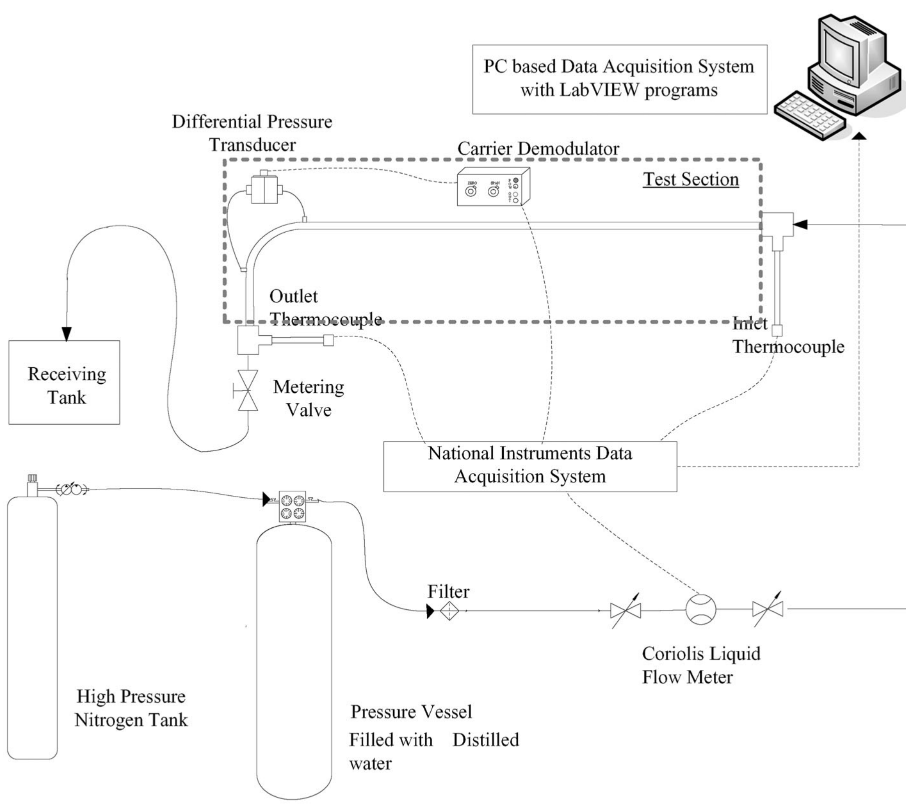


(b)

**Figure 1.** Experimental setup for (a) straight tube; (b) 90° and 45° elbows.

Table 1. Specification of the straight stainless tested tubes with different diameters.

| | Value | | |
|---|---|---|---|
| Parameters | Tube 1 | Tube 2 | Tube 3 |
| Inner diameter, $D_i$ (mm) | 0.60 | 0.80 | 4.50 |
| Outer diameter, $D_o$ (mm) | 0.80 | 1.60 | 6.40 |
| Average Roughness, $\varepsilon_{avg}$ (μm) | 0.48 | 0.99 | 0.76 |

respectively. In that study, the two-phase flow pressure drop correlation was developed in terms of curvature multiplier to the straight tube two-phase pressure drop. However, the single-phase pressure drop experiment was not mentioned in that study.

Mortazavi [13] studied the two-phase pressure drop in proton exchange membrane fuel cell flow channel bends experimentally. A 90° sharp-edged bend was fabricated across a square channel with a hydraulic diameter of 1 mm. Experiments were conducted by supplying air and hydrogen into the flow channel bends. In that study, the two-phase flow pressure drop model was developed in terms of the gas minor loss. To predict the gas minor loss, a correlation for the loss coefficient was obtained based on the gas single-phase pressure drop in the laminar region.

Therefore, the objectives of this study are to investigate the friction factor inside the 45° and 90° mini-elbows and compare the current data with the existing correlations.

## Experimental method

The experimentation for this study was performed using a relatively simple but highly effective apparatus. The apparatus used was designed with the intention of conducting highly accurate pressure drop measurements. The apparatus consists of four major components. These are the fluid delivery system, the flowmeter banks, the test section assembly, and the data acquisition system. An overall schematic for the experimental test apparatus is shown in Figure 1.

The fluid delivery system consists of a high-pressure cylinder filled with ultra-high purity nitrogen in combination with a stainless-steel pressure vessel. After the working fluid passes through the apparatus, it is collected into a sealed container. The working fluid, distilled water is stored in the stainless-steel pressure vessel. As the pressurized nitrogen is fed into the pressure vessel, the working fluid is forced up a stem extending to the bottom of the vessel, out of the pressure vessel, and through the flowmeter and test section. After passing through the flowmeter, fluid enters the test section assembly. The accuracy of the mass flow rate of the Coriolis flowmeter was calibrated by factory within ±1.75%. Based on the flow measurement, the Reynolds number range for this study was around 800 to 10,000. The test section assembly contains the test section as well as the equipment necessary for the measurement of inlet and outlet fluid temperature and pressure drop. The test section is placed on an experimental table and a level is used to keep the test section in a horizontal position.

In this study, the test sections included three straight tubes, three 90° elbows, and three 45° elbows. They are made of Grade 304 stainless steel and with inner diameters of 0.6 mm, 0.8 mm, and 4.5 mm, respectively. The three straight tubes with three different diameters were used for verification of the experimental setup only. Table 1 lists the specification of the three straight stainless tubes. As shown in Figure 1a, the straight tube is arranged as the test section and the length-to-diameter ratio ($x/D_i$) between the two pressure taps arranged on the top of the straight tube was 200.

For studying the loss coefficients of mini-elbows, those elbows were fabricated by bending the same batch of straight tubes at the angles of 45° and 90°. As shown in Figure 1b, the whole 90° elbow tested tube includes the preceding straight tube ($x/D_i >$ 160), the bend, and the succeeding straight tube without any joint. For testing the 45° elbow, the whole 90° elbow tested tube is replaced by the 45° elbow tested tube. Because the pressure drop measurement points are directly arranged at the inlet and outlet of the elbows, the measured pressure drop only reflects pressure loss inside the elbow itself. In general, the measured value was less than the "equivalent pressure drop" calculated in terms of the equivalent length of preceding and succeeding straight tube and the total pressure drop through the preceding, elbow, and succeeding straight tubes [3]. The specification of mini-scale elbows is shown in Table 2. In the table, the average roughness was measured by Atomic Force Microscope (AFM, XE7, Park-Systems).

Figure 2 shows the stainless-steel pressure taps for three different diameter tubes and elbows. As shown in Figure 2, the 1.6 mm outer diameter bulged tube is used as the pressure tap for the 4.5 mm tested tube. The 0.45 mm outer diameter infusion needle is used as the pressure tap for the 0.8 mm tested tube. For the smaller 0.6 mm tube, a 0.45 mm hole is first drilled on the top of the tested tube and then the "hole" part of the tested tube is inserted laterally through a plastic tube which one end is sealed and another end is connected to the pressure transducer. So, the fluid

**Table 2.** Specification of the tested elbows with different diameters and angles.

| Parameters | Elbow 1 | Elbow 2 | Elbow 3 | Elbow 4 | Elbow 5 | Elbow 6 |
|---|---|---|---|---|---|---|
| Inner diameter, $D_i$ (mm) | 0.60 | 0.80 | 4.50 | 0.60 | 0.80 | 4.50 |
| Outer diameter, $D_o$ (mm) | 0.80 | 1.60 | 6.40 | 0.80 | 1.60 | 6.40 |
| Angle, $\alpha$ | 45° | | | 90° | | |
| Curvature radius for the elbow, R (mm) | 6.00 | 7.60 | 41.30 | 6.00 | 7.60 | 41.30 |
| Curvature ratio for the elbow , $R/D_i$ | 10.00 | 9.30 | 9.20 | 10.00 | 9.30 | 9.20 |
| Average roughness, $\varepsilon_{avg}$ (μm) | 0.48 | 0.99 | 0.76 | 0.48 | 0.99 | 0.76 |

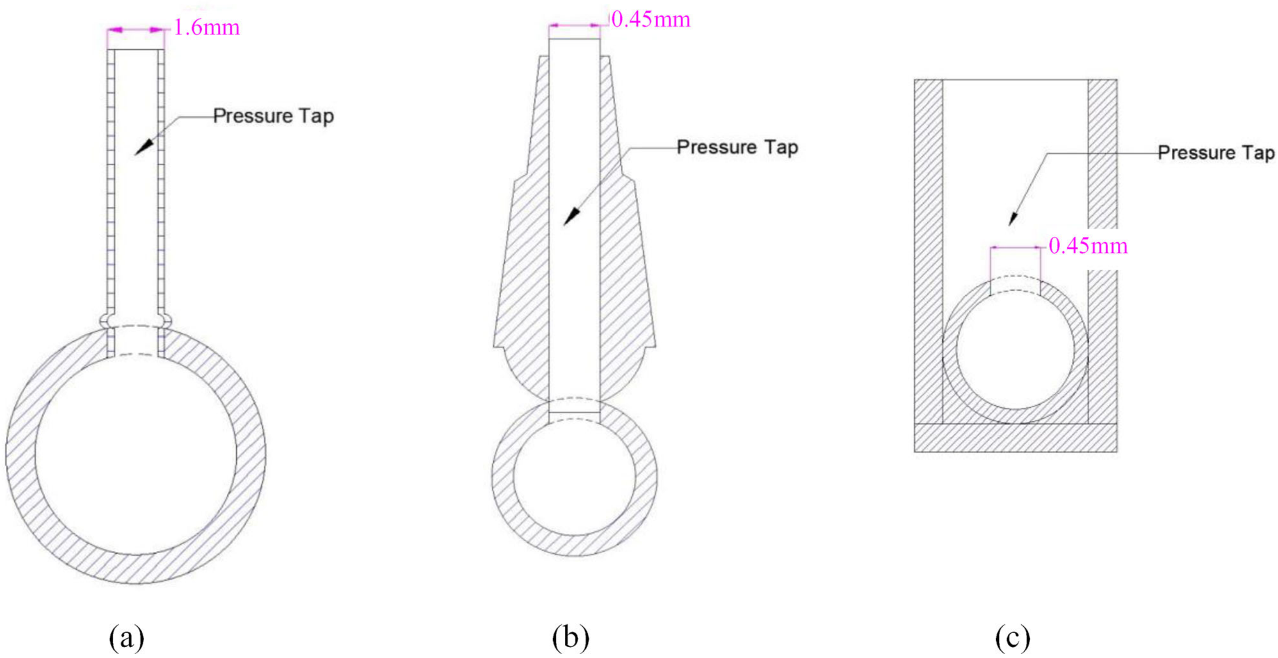


**Figure 2.** Pressure taps for different diameter tubes or elbows: (a) 4.5 mm; (b) 0.8 mm; (c) 0.6 mm.

pressure from the tube hole can be measured through the plastic tube.

For the pressure drop measurements, based on Ghajar et al. [14], careful attention was paid to the sensitivity of the diaphragms of the pressure transducer. From the manufacturer, the accuracy of the Validyne DP15 pressure transducer is given as ±0.25% of the full scale reading of each diaphragm used. In this study, it was confirmed again that different ranging diaphragms would generate different results even in the same Reynolds number range. To ensure the measurement accuracy, a suitable diaphragm was selected based on the Reynolds number range. Calibrations for pressure transducer were performed before each test run. For the calibration purpose, Validyne hand-held pressure calibrator (T140) with an accuracy of 0.05% FS was used.

As shown in Figure 1, inlet and exit bulk temperatures were measured by means of thermocouple probes (Omega TMQSS-020U-6) placed before and after the test section, respectively. They were calibrated by a PolyScience constant temperature circulating bath with an accuracy within ±0.2 °C. In this study, the inlet and exit bulk temperatures were just used for ensuring the test section is operating under the isothermal condition.

For data acquisition, a National Instruments Compact DAQ data collecting system was used. All digital signals from the flow meters, thermocouples, and pressure transducer were acquired and recorded by the Windows-based PC with a self-developed LabVIEW program. The uncertainty analyses of the overall experimental procedures using the method of Kline and McClintock [15] showed that there is a maximum of ±6% uncertainty for the friction factor calculation. Table 3 lists the uncertainties of the parameters used to obtain the uncertainty of friction factor.

## Results and discussion

Based on the careful consideration of the sensitivity of pressure transducer, the measurements of friction factor were also verified by comparing the friction factor data of the horizontal straight tubes with three

**Table 3.** Uncertainties of the parameters used in this study.

| Parameters | Uncertainty |
|---|---|
| Pressure drop, $\Delta P$ | 0.25% |
| Tube diameter, $D_i$ | 0.11% |
| Tube length between the pressure drop measurement points, L | 0.11% |
| Flow rate, Q | 1.75% |
| Density, $\rho$ | 0.7% |

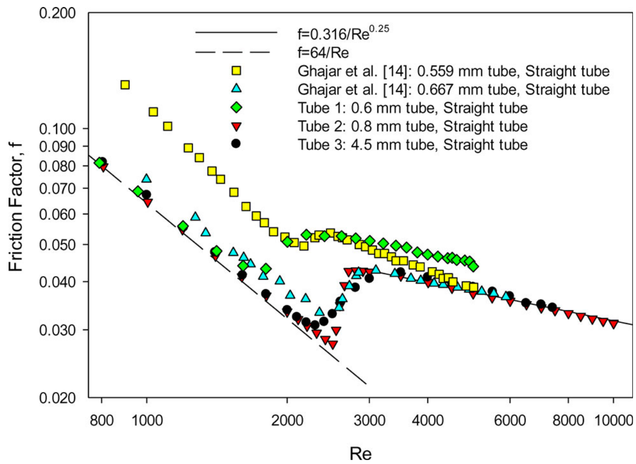


**Figure 3.** Comparison of present friction factor data for the 0.6 mm, 0.8 mm, and 4.5 mm diameters stainless steel tubes with classical equations and experimental data of Ghajar et al. [14].

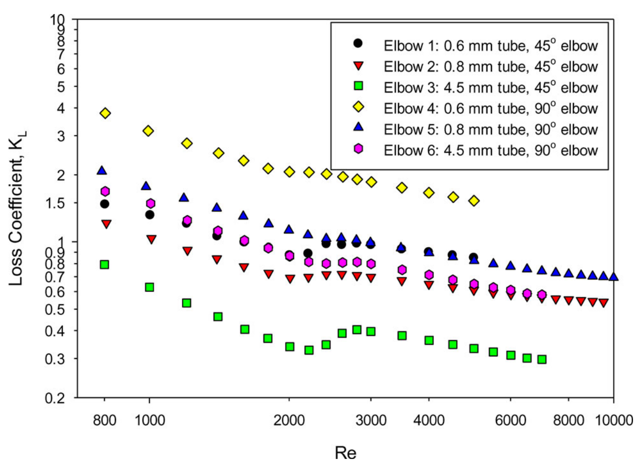


**Figure 4.** Comparison of all loss coefficient data for the 45° and 90° elbows.

different diameters with the classical friction factor equations for laminar and turbulent flows.

As seen in Figure 3, the friction factor data of the 4.5 mm and 0.8 mm tubes compare very well with the classical fully developed friction factor equations in the laminar ($f = 64/Re$) and turbulent (Blasius equation, $f = 0.316/Re^{0.25}$) regions [16]. Hence, the entire experimental setup for the pressure drop measurements was verified to be reliable. For the smaller 0.6 mm tube, the friction factor profile was shifted up from the classical laminar and turbulent equations. In the figure, it was also observed that the present 0.6 mm tube data fall in between the friction factor data of Ghajar et al. [14] with similar diameters, 0.559 mm and 0.667 mm. Referring to Ghajar et al. [14], the shift-up behavior observed in the smaller tube diameters might be due to the potential effect of surface roughness in the smaller tube diameters.

After the verifications of the experimental setup, the pressure drop measurements under isothermal condition for the 45° and 90° elbows with the diameters of 0.6 mm, 0.8 mm, and 4.5 mm were conducted. Figure 4 clearly shows the loss coefficient characteristics for all six elbows (Elbows 1 to 6). In the figure, it is shown that the loss coefficient data of the Elbows 4 to 6 (i.e., the 90° elbow) are basically higher than the data of the Elbows 1 to 3 (i.e., 45° elbow). It means that a larger angle leads to a larger pressure loss in the elbow. Comparing the same elbow angle (45° or 90° elbow), it is also observed that the tube diameter influences the loss coefficient. The loss coefficient is increased by the decrease of diameter due to the increase of pressure drop in a narrower flow path.

Regarding the loss coefficient characteristics, the 45° elbow characteristics are similar to the friction factor characteristics of straight tube from laminar to turbulent region. As seen in the figure, in the lower Reynolds number range ($800 \leq Re < 2{,}200$), the data trend first moves along an inclined straight line to a lower critical point of around 2,000 and then rises abruptly until the upper critical point (i.e., $Re \approx 2{,}800$). The lower critical points of the smaller diameter (0.6 mm and 0.8 mm) elbows located at Reynolds number of 2,000 is earlier than that of 4.5 mm elbow located at the Reynolds number of 2,200. After the critical region, the data trend continues to incline with the increase of Reynolds number. Keulegan and Beij [17] also observed the critical region in the bending tubes and stated the lower critical number increased as the curvature ratio increased. For the current data, the critical region was not obvious in the 90° elbows.

Figure 5 shows the comparison of the loss coefficient data for the 45° elbows with the values calculated by the 2-K and 3-K correlations. Moreover, the fixed loss coefficient value of 0.21, for the one-inch 45° long-radius flanged elbow from White [1] is also plotted in the figure. Referring to Hooper [5], the 2-K equation is expressed as:

$$K_L = K_1/Re + K_\infty(1 + 1/D_{i,\,in}) \quad (1)$$

where Re is the Reynolds number, $D_{i,\ in}$, in is the internal diameter in inches, for 45° long radius elbow

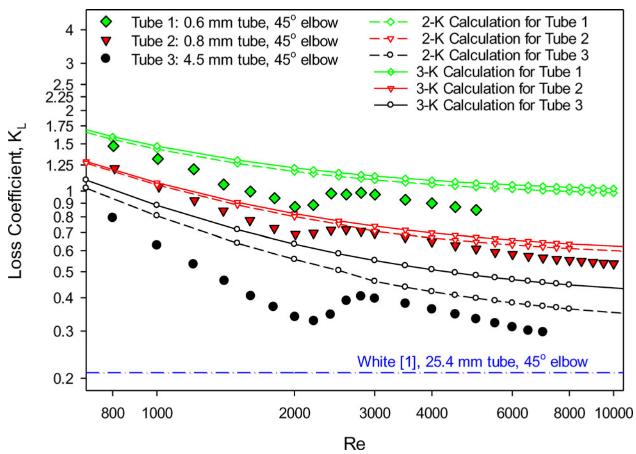


**Figure 5.** Comparison of present loss coefficient data for the 45° elbows with those values calculated from the 2-K and 3-K correlations.

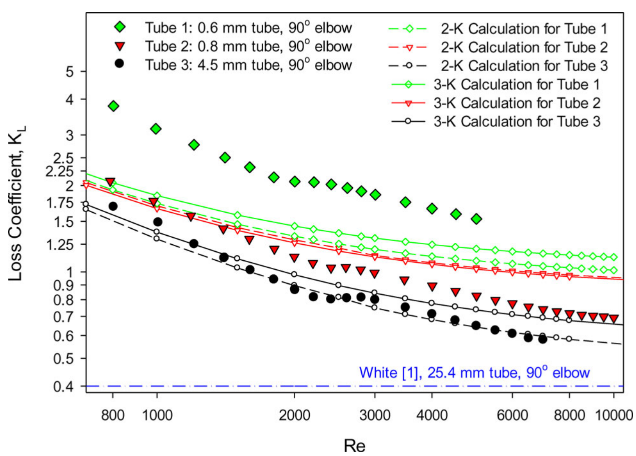


**Figure 6.** Comparison of present loss coefficient data for the 90° elbows with those values calculated by the 2-K and 3-K correlations.

($R/D_i = 1.5$), $K_1 = 500$, $K_\infty = 0.15$; for 90° long radius elbow ($R/D_i = 1.5$), $K_1 = 800$, $K_\infty = 0.2$.

Referring to Darby and Chhabra [4], the 3-K equation is expressed as:

$$K_L = K_1/Re + K_i(1 + K_d/D_{n,in}{}^{0.3}) \tag{2}$$

where Re is the Reynolds number, $D_{n,in}$ is the nominal diameter in inches, for 45° long radius elbow ($R/D_i = 1.5$), $K_1 = 500$, $K_i = 0.052$, $K_d = 4.0$; for 90° long radius elbow ($R/D_i = 1.5$), $K_1 = 800$, $K_i = 0.071$, $K_d = 4.2$.

In Figure 5, for the 45° elbows, the 2-K and 3-K curves are smooth curves without showing the critical region of the current experimental data. Those calculated curves basically deviate from the current experimental data. The 2-K and 3-K correlations overpredict the current data, especially, for the 4.5 mm elbow. For the 4.5 mm elbow, the maximum deviations predicted by 2-K and 3-K methods are 38.8% and 46.5%, respectively. The traditional correlations were developed for the larger pipe diameters and based on the elbows with smaller curvature ratio of 1.5. Therefore, the elbow size and the curvature ratio need to be considered when developing a suitable correlation for the mini-elbows. In the figure, it is also seen that the fixed value of White [1] is much lower than the current values for the 45° elbows data and the fixed value cannot represent the loss coefficient behaviors in the entire Reynolds number range. Therefore, the fixed loss coefficient value is not suitable to use for the mini scale 45° elbows.

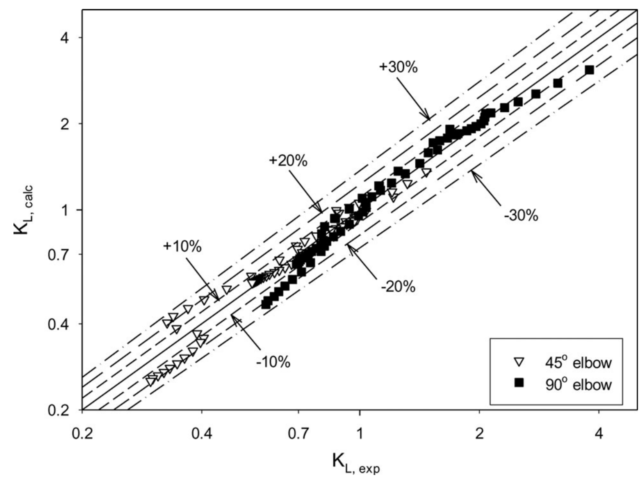


**Figure 7.** Comparison between experimental loss coefficients and the proposed correlation, Eq. (3).

Figure 6 shows the comparison of the loss coefficient data for the 90° elbows with the values calculated by the 2-K and 3-K correlations. Moreover, the fixed loss coefficient value of 0.4, for the one-inch 90° long-radius flanged elbow from White [1] is also plotted in the figure. In the figure, it can be seen that the 2-K and 3-K curves are relatively close to the 4.5 mm data. For the 4.5 mm elbow, the maximum deviation between the 2-K and 3-K predicted values and the experimental data is less than ±20%. However, those calculated curves for 0.6 mm and 0.8 mm elbows obviously deviate from the current experimental data. Therefore, an accurate correlation for the 90° mini-elbows is developed in this study. In Figure 6, it is also seen that the fixed value of White [1] is much lower than the current 90° elbows data and the fixed value cannot represent the loss coefficient behaviors in the entire Reynolds number range. Therefore, the fixed loss coefficient value is not suitable to use for the mini scale 90° elbows, either.

In the development of correlation, a total of 128 isothermal experimental data points (62 data points for the 45° elbows and 66 data points for the 90° elbows) were used. For correlating the loss coefficient data in the entire flow regime ($800 < \mathrm{Re} < 10{,}000$), a correlation form similar to the 3-K equation [4] and two sets of parameters for the 45° and 90° elbows are proposed as follows:

$$K_L = \frac{a}{\mathrm{Re}} + b\left(1 + \frac{c}{D_{i,mm}^{n}}\right) \tag{3}$$

where $a = 487$, $b = 0.17$, $c = 1.3$, $n = 1.9$ for the 45° elbow ($R/D_i \approx 10$) and $a = 1{,}310$, $b = 0.28$, $c = 0.24$, $n = 5.6$ for the 90° elbow ($R/D_i \approx 10$). For 45° and 90° elbows ($R/D_i \approx 10$), the applicable range of the diameters of Eq. (3) is $0.6\,\mathrm{mm} \le D_i \le 4.5\,\mathrm{mm}$.

Eq. (3) gives a representation of the experimental data to within +25.6% to −19.5%. The average deviation between the results predicted by the correlation and the experimental data is 7.3%; 2% (3 data points) were predicted with ±20–30% deviation, 23% (29 data points) were predicted with ±10–20% deviation, 75% (96 data points) were predicted with less than ±10% deviation. Figure 7 compares the predicted loss coefficients obtained from the proposed correlation with measurements. Compared to 2-K and 3-K correlations, Eq. (3) can predict the loss coefficients data of the current mini-elbows with better accuracy.

## Conclusions

In this study, an experimental setup was designed and verified for the measurements of pressure drop in the horizontal straight tubes and mini-elbows under isothermal boundary condition. The following conclusions were drawn from the experimental results:

- The pressure drop in the 90° elbow was larger than that of the 45° elbow.
- For either 45° or 90° elbow, a decrease in the tube diameter induced an increase of loss coefficient.
- A critical region was observed in the loss coefficient characteristics of 45° elbow, but this was not obvious in the 90° elbow.
- In general, the 2-K and 3-K methods did not predict the loss coefficients of the 45° and 90° elbows with good accuracy.
- An accurate correlation for the prediction of loss coefficients of the mini-elbows was developed in this study.

In the future study, it is recommended to analyze the potential effect of the surface roughness and the curvature ratio on pressure drop and flow behaviors inside the horizontal, vertical-upward, and vertical-downward mini-elbows. Furthermore, the changes of the pressure drop of the tube lengths before and after the mini-elbow should be observed and analyzed. Based on the experimental data, the proposed loss coefficient correlation can be generally suitable for more mini-elbows with different roughness and curvature ratio.

## Funding

This research is supported by the Institute for the Development and Quality, Macau.

## Notes on contributors

*Hou Kuan Tam* received his PhD in 2013 from University of Macau, Department of Electromechanical Engineering, Macau, China. His research interests include internal flow heat transfer and pressure drop, heat transfer enhancement, fire protection engineering, and the application of computation intelligence in thermal engineering problems.

*Jia Qi Ji* received his MS in 2019 from University of Macau, Department of Electromechanical Engineering, Macau, China. His research interest is the internal flow pressure drop in fittings.

*Lap Mou Tam* received his PhD in 1995 from Oklahoma State University, School of Mechanical and Aerospace Engineering, Stillwater, Oklahoma, USA. In 1996, he joined the University of Macau as an assistant professor and is currently a full professor in the department of electromechanical engineering at the University of Macau, Macau, China. In 2001, he was appointed by the University of Macau to serve as the chairman of board of directors in the Institute for the Development and Quality, a nonprofit institute providing mechanical- and electromechanical-related engineering services to the public. His research interests include single and multiphase heat transfer, chaos, fire engineering, and indoor air quality. He is a senior member of the Chinese Mechanical Engineering Society.

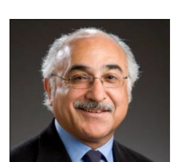

*Afshin J. Ghajar* is Regents Professor and John Brammer Professor in the School of Mechanical Engineering and Aerospace Engineering at Oklahoma State University. He is a Fellow of the American Society of Mechanical Engineers (ASME) and the

American Society of Thermal and Fluids Engineers (ASTFE). He is a Registered Professional Engineer in the State of Oklahoma. Professor Ghajar has received countless teaching/service awards, such as the 75th Anniversary Medal of the ASME Heat Transfer Division, the ASME ICNMM Outstanding Leadership Award, and the Donald Q. Kern Award, among others. His research work has resulted in over 250 publications including professional journals, reports, books, peer-reviewed conference papers or symposium proceedings. His research achievements have also been documented by a large number of presentations as well as keynote and invited lectures all over the world. A 2020 study conducted by Ionnidis et al. of Stanford University [Updated science-wide author databases of standardized citation indicators (plos.org)], ranked nearly 160,000 scientists of all disciplines based on citations to their work over their career and for the year 2019, Professor Ghajar ranked in the top 1.3% of researchers in Mechanical Engineering and Transports category. He currently serves as the Editor-in-Chief of *Heat Transfer Engineering Journal* and is the Heat Transfer Series Editor for CRC Press (he has edited 13 books to date). He is the coauthor of two popular textbooks, *Heat and Mass Transfer – Fundamentals and Applications*, 6th Edition (2020), and *Fundamentals of Thermal-Fluid Sciences*, 6th Edition (2022), both published by McGraw-Hill; and the author of *Two-Phase Gas-Liquid Flow in Pipes with Different Orientations*, Springer Briefs in Applied Sciences and Technology, published by Springer 2020, and *Single- and Two-Phase Flow Pressure Drop and Heat Transfer in Tubes*, Mechanical Engineering Series, published by Springer, 2022.

## References

[1] F. M. White, *Fluid Mechanics*, 4th ed. New York: McGraw-Hill, 1999.

[2] Y. A. Cengel and J. M. Cimbala, *Fluid Mechanics: Fundamentals and Applications*, 3rd ed. New York: McGraw-Hill, 2014,

[3] P. L. Spedding, E. Benard, and G. M. McNally, "Fluid flow through 90 degree bends," *Dev. Chem. Eng. Mineral Process*, vol. 12, no. 1-2, pp. 107–128, 2008. DOI: 10.1002/apj.5500120109.

[4] R. Darby and R. P. Chbabra, *Chemical Engineering Fluid Mechanics*, 3rd ed. Boca Raton, Florida: CRC Press, 2016,

[5] W. B. Hooper, "The two-K method predicts head losses in pipe fittings," *Chem. Eng.*, vol. 88, pp. 96–100, Aug. 1981.

[6] W. B. Hooper, "Calculate head loss caused in pipe size," *Chem. Eng.*, vol. 95, pp. 89–92, Nov. 1988.

[7] R. Darby, "Correlate pressure drops through fittings," *Chem. Eng.*, vol. 108, no. 4, pp. 127–130, 2001. https://www.researchgate.net/publication/287851085.

[8] W. Al-Tameemi and P. Ricco, "Pressure-loss coefficient of 90 deg sharp-angled miter elbows," *ASME J. Fluids Eng.*, vol. 140, no. 6, pp. 061102, 2018. DOI: 10.1115/1.4038986.

[9] K. Gasljevic and E. F. Matthys, "Friction and heat transfer in drag-reducing surfactant solution flow through curved pipes and elbows," *Eur. J. Mech. B/Fluids*, vol. 28, no. 5, pp. 641–650, 2009. DOI: 10.1016/j.euromechflu.2009.04.003.

[10] P. L. Spedding, E. Benard, and N. M. Crawford, "Fluid flow through a vertical to horizontal 90° elbow bend III three phase flow," *Exp. Therm. Fluid Sci.*, vol. 32, no. 3, pp. 827–843, 2008. DOI: 10.1016/j.expthermflusci.2007.10.002.

[11] L. Hsu, Y. Chen, C. Chyu, and C. C. Wang, "Two-phase pressure drops and flow pattern observations in 90 bends subject to upward, downward and horizontal arrangements," *Exp. Therm. Fluid Sci.*, vol. 68, pp. 484–492, Nov. 2015. DOI: 10.1016/j.expthermflusci.2015.06.012.

[12] A. T. Autee and S. V. Giri, "Experimental study on two-phase flow pressure drop in small diameter bends," *Perspect. Sci.*, vol. 8, pp. 621–625, 2016. DOI: 10.1016/j.pisc.2016.06.038.

[13] M. Mortazavi, "Two-phase flow pressure drop in PEM fuel cell flow channel bends," *Int. J. Multiphase Flow*, vol. 143, pp. 103759, Oct. 2021. DOI: 10.1016/j.ijmultiphaseflow.2021.103759.

[14] A. J. Ghajar, C. C. Tang, and W. L. Cook, "Experimental investigation of friction factor in the transition region for water flow in minitubes and microtubes," *Heat Transf. Eng.*, vol. 31, no. 8, pp. 646–657, 2010. DOI: 10.1080/01457630903466613.

[15] S. J. Kline and F. A. McClintock, "Describing uncertainties in single sample experiments," *Mech. Eng.*, vol. 75, no. 1, pp. 3–8, 1953.

[16] Y. A. Cengel and A. J. Ghajar, *Heat and Mass Transfer: Fundamentals & Applications*, 6th ed. New York: McGraw-Hill Education, 2020.

[17] G. H. Keulegan and K. H. Beij, "Pressure losses for fluid flow in curved pipes," *J. Res. Natl. Bur. Stan.*, vol. 18, no. 1, pp. 89–114, 1937. DOI: 10.6028/jres.018.049.